Journal of Physics: Conference Series **455** (2013) 012036 doi:10.1088/1742-6596/455/1/012036

CP violation at LHCb

Olaf Steinkamp ***on behalf of the LHCb Collaboration***

Physik-Institut der Universität Zürich, Winterthurerstrasse 190, 8057 Zürich, Switzerland

E-mail: olafs@physik.uzh.ch

Abstract. Precision measurements of *CP* violating observables in the mixing and decay of B mesons provide excellent opportunities to search for possible contributions from New Physics beyond the Standard Model. In these proceedings, key measurements pursued by the LHCb collaboration at CERN's Large Hadron Collider (LHC) are described. Results obtained from the analysis of data collected in 2011 already match or even surpass the measurements of previous experiments in their precision. All results obtained so far are compatible with Standard Model predictions, hints for possible deviations reported by previous experiments are not confirmed. All results are dominated by statistical uncertainties and significant improvements are expected from analysing larger data sets. The total integrated luminosity accumulated by LHCb has already been tripled in 2012 and is expected to more than double again in the data taking period following the first long shutdown of the LHC. A comprehensive upgrade of the LHCb apparatus is then foreseen for the second long shutdown of the LHC accelerator in 2018/2019. The main goals of the LHCb upgrade are to operate the experiment at higher instantaneous luminosities and to improve further the trigger efficiency for heavy quark decays to purely hadronic final states.

1. Introduction

The main goal of the LHCb experiment [1] at CERN's Large Hadron Collider (LHC) is the search for possible contributions from physics beyond the Standard Model ("New Physics") by performing precision measurements of *CP* violating observables and rare decays of hadrons containing a b quark or a c quark. The LHCb detector and its performance in the first LHC runs, as well as key measurements of rare b and c decays, are described in another contribution to these proceedings [2]. Here, we will concentrate on measurements of *CP* violating observables. Unless mentioned otherwise, the measurements have been performed using the full 2011 data set, corresponding to an integrated luminosity of 1.0 fb^{-1} of pp collisions collected at a centre of mass energy of 7 TeV.

The only source of *CP* violation in the Standard Model of particle physics is a single complex phase in the Cabbibo-Kobayashi-Maskawa (CKM) matrix [3, 4], which parametrises the mixing between the quark families in charged current interactions. For the case of three quark families, the CKM matrix is fully described by four independent real parameters, namely three rotation angles and one complex phase. A non-zero value of this complex phase can induce *CP* violating asymmetries in processes in which two or more amplitudes with different weak phases interfere. Often, one of the interfering amplitudes involves loop diagrams with internal quark lines, such as box or penguin diagrams. Heavy new particles, which are predicted by most New Physics models, can then appear in the internal lines of these loop diagrams and modify the observed asymmetries with respect to Standard Model predictions. Precision measurements of these

asymmetries therefore test the Standard Model and can reveal the presence of New Physics. Since these measurements probe the effect of virtual particles in internal loop diagrams, their sensitivity extends to much higher mass scales than direct searches for new particles, which are limited to the centre of mass energy of the accelerator at which the measurement is performed. Moreover, the pattern of observed deviations from Standard Model predictions can hint at the underlying dynamics of the New Physics at play. The B meson systems ($B^{\pm}$, $B^0/\overline{B}^0$ and $B_s^0/\overline{B}_s^0$) give rise to a rich phenomenology with a wide range of observables for which precise Standard Model predictions are available. Particularly high sensitivity to possible contributions from New Physics can be achieved in processes where the predicted asymmetry in the Standard Model is small.

The CKM picture gives rise to three mechanisms that can lead to *CP* violating asymmetries:

CP **violation in mixing** in the $B^0\overline{B}^0$ and $B_s^0\overline{B}_s^0$ systems is caused by the interference of box diagrams with different internal quark lines. The mixing phase in the $B_s^0\overline{B}_s^0$ system is predicted with good precision to be close to zero in the Standard Model and is therefore particularly sensitive to possible contributions from New Physics.

CP **violation in decay** is caused by the interference of decay diagrams with different weak phase and different strong phase leading to the same final state. This is the only possible source of *CP* violation for charged B mesons. In general, the poorly known strong phases limit the precision with which the weak phase can be extracted from the measured asymmetry. There are, however, cases in which the weak phase can be cleanly extracted using a combination of several related decay modes and exploiting symmetries of the strong interaction between these modes.

CP **violation in the interference of mixing and decay** of B^0 or B_s^0 mesons to a final state that is accessible to both the $B_{(s)}^0$ meson and its antiparticle is caused by the interference of the direct decay amplitude of a $B_{(s)}^0$ meson to the given final state and the process where the $B_{(s)}^0$ meson first mixes to a $\overline{B}_{(s)}^0$, which then decays to the same final state. A prominent example is the "golden" decay mode $B^0 \to J/\psi K_S^0$, which allowed the precise measurement of the mixing phase $\sin 2\beta$ in the $B^0\overline{B}^0$ system by the B factories BaBar [5] and Belle [6].

In the following, we will encounter examples of all three types of *CP* violation.

2. Semileptonic Asymmetry

Second-order weak transitions (box diagrams) induce particle-antiparticle mixing in the $K^0\overline{K}^0$, $D^0\overline{D}^0$, $B^0\overline{B}^0$ and $B_s^0\overline{B}_s^0$ systems. The time evolution of the coupled particle–antiparticle system can be described by an effective 2×2 Schrödinger equation of the form

$$-i\frac{\partial}{\partial t}\begin{pmatrix} B_s^0 \\ \overline{B}_s^0 \end{pmatrix} = H \cdot \begin{pmatrix} B_s^0 \\ \overline{B}_s^0 \end{pmatrix} = \begin{pmatrix} M_{11} - \frac{i}{2}\Gamma_{11} & M_{12} - \frac{i}{2}\Gamma_{12} \\ M_{12}^\star - \frac{i}{2}\Gamma_{12}^\star & M_{22} - \frac{i}{2}\Gamma_{22} \end{pmatrix} \cdot \begin{pmatrix} B_s^0 \\ \overline{B}_s^0 \end{pmatrix}$$

(and similar for the other neutral meson–antimeson systems). The eigenstates of the effective Hamiltonian H are the heavy and light mass eigenstates, B_H and B_L, which have well defined masses, m_H and m_L, and lifetimes, Γ_H and Γ_L. Relevant observables are the mass difference $\Delta m_s \equiv m_H - m_L$ and the lifetime difference $\Delta\Gamma_s \equiv \Gamma_H - \Gamma_L$. Note that Δm_s is positive by definition, whereas $\Delta\Gamma_s$ can be positive or negative. Particle-antiparticle mixing is described by the off-diagonal elements of H. A relative phase ϕ_M between M_{12} and Γ_{12} induces *CP* violation in mixing, implying that the probability for the transition $B_s^0 \to \overline{B}_s^0$ is different from the probability for the transition $\overline{B}_s^0 \to B_s^0$. This *CP* asymmetry can be measured in the time-integrated semileptonic asymmetry

$$a_{\rm sl}^s \equiv \frac{\Gamma(\overline{B}_s^0 \to \ell^+ X) - \Gamma(B_s^0 \to \ell^- X)}{\Gamma(\overline{B}_s^0 \to \ell^+ X) + \Gamma(B_s^0 \to \ell^- X)} = \frac{\Delta\Gamma_s}{\Delta m_s}\tan\phi_M.$$

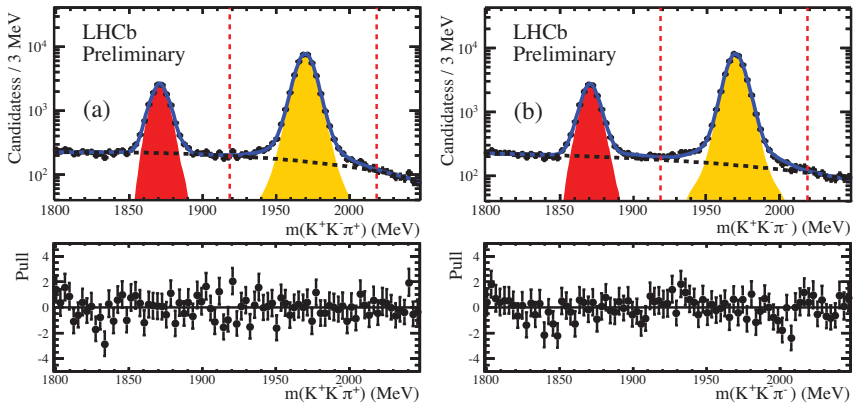

Figure 1. Invariant mass distributions for (a) $K^+K^-\pi^+$ candidates and (b) $K^+K^-\pi^-$ candidates for magnet up polarity, with $m(K^+K^-)$ within ± 20 MeV/c^2 of the ϕ meson mass.

In the Standard Model, the phase ϕ_M in the $B_s^0\overline{B}_s^0$ system is small and the semileptonic asymmetry is predicted to be $a^s_{\rm sl} = (1.9 \pm 0.3) \times 10^{-5}$ [7]. The corresponding asymmetry in the $B^0\overline{B}^0$ system is predicted to be $a^d_{\rm sl} = (4.1 \pm 0.6) \times 10^{-4}$ [7]. Measurements of $a^d_{\rm sl}$ reported by the B factories [8, 9, 10] and by D0 [11] agree with the Standard Model prediction. The D0 collaboration, however, also reported a measurement of the asymmetry in the rate of like-sign muon pairs, $A_{\mu\mu} \approx 0.6 \cdot a^d_{\rm sl} + 0.4 \cdot a^s_{\rm sl}$, which yielded an anomalously large value [12].

LHCb has reported a preliminary measurement of $a^s_{\rm sl}$ [13] using the decay $B_s^0 \to D_s^-\mu^+X$ with $D_s^- \to \phi\pi^-$ and $\phi \to K^+K^-$. No flavour tagging was employed to determine the initial flavour of the B_s^0 meson at its production. The measured raw asymmetry is then

$$A_{\rm raw} \equiv \frac{N(D_s^-\mu^+X) - N(D_s^+\mu^-X)}{N(D_s^-\mu^+X) + N(D_s^+\mu^-X)} = \frac{a^s_{\rm sl}}{2} + \kappa \cdot \left[a_{\rm p} - \frac{a^s_{\rm sl}}{2}\right],$$

where $a_{\rm p}$ is the $B_s^0 - \overline{B}_s^0$ production asymmetry and

$$\kappa \equiv \frac{\int e^{-\Gamma_s t}\,\cos(\Delta m_s t)\,\epsilon(t)\,dt}{\int e^{-\Gamma_s t}\,\cosh(\Delta\Gamma_s t/2)\,\epsilon(t)\,dt}$$

is a dilution factor due to $B_s^0 - \overline{B}_s^0$ oscillation, with $\epsilon(t)$ describing the reconstruction efficiency as a function of the decay time. The large oscillation frequency leads to a very small value of κ in the $B_s^0\overline{B}_s^0$ system, with $\kappa \approx 2 \times 10^{-3}$ for the LHCb decay time acceptance. Therefore, even a production asymmetry $a_{\rm p}$ of a few percent would be washed out to a negigible level compared to the current statistical precision of the measurement.

Candidates were selected using a trigger that first required a muon with significant transverse momentum, followed by two inclusive selections that made use either of the topology of a displaced decay vertex or the kinematic reconstruction of $\phi \to K^+K^-$ decays. To minimize and control potential detector asymmetries, the polarity of the LHCb dipole magnet was reversed several times throughout the data taking period. The complete analysis was performed separately for these two subsets of the data and the two results were then averaged to obtain the final result. Detection asymmetries largely cancel due to this averaging. Residual detection asymmetries were estimated from data, using dedicated control samples. Combinatorial background was subtracted statistically by fitting the $K^+K^-\pi^+$ invariant mass distributions as shown in Fig. 1 for candidates collected with one of the two magnet polarities. Other backgrounds are small and accounted for as part of the systematic uncertainties.

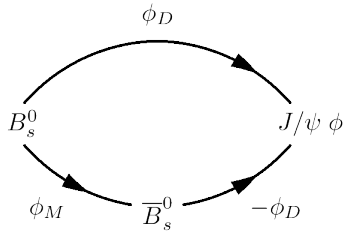

Figure 2. Illustration of weak phases in the interference of mixing and decay for $B_s^0 \to J/\psi\phi$. See the text for further explanations.

The measured asymmetry is $a_{\rm sl}^s = (0.24 \pm 0.54(\text{stat}) \pm 0.33(\text{syst})) \times 10^{-2}$ and agrees with the Standard Model prediction. The precision of the measurement is limited by the statistical uncertainty. The systematic uncertainty is dominated by the statistical uncertainty on the determination of efficiency ratios and can be expected to decrease with larger control samples.

3. *CP* violation in $B_s^0 \to J/\psi\phi$ and $B_s^0 \to J/\psi\pi^+\pi^-$

The final state $J/\psi\phi$ is accessible to both B_s^0 and $\overline{B}_s^0$. As illustrated in Fig. 2, the interference between the decay amplitudes and the $B_s^0 - \overline{B}_s^0$ mixing amplitude can give rise to a *CP* violating phase

$$\phi_s = \phi_M - 2\phi_D,$$

where ϕ_M is the $B_s^0 - \overline{B}_s^0$ mixing phase discussed in the previous section and ϕ_D is the weak decay phase. In the Standard Model, ϕ_D is very small, resulting in a precise prediction of $\phi_s = 0.036 \pm 0.002$ rad [15]. A measurement of ϕ_s is interesting since it is very sensitive to possible contributions from New Physics in $B_s^0 - \overline{B}_s^0$ mixing.

The experimental determination of ϕ_s proceeds through the measurement of the time-dependent *CP* asymmetry

$$A_{CP}(t) \equiv \frac{\frac{\partial\Gamma}{\partial t}(\overline{B}_s^0 \to J/\psi\phi) - \frac{\partial\Gamma}{\partial t}(B_s^0 \to J/\psi\phi)}{\frac{\partial\Gamma}{\partial t}(\overline{B}_s^0 \to J/\psi\phi) + \frac{\partial\Gamma}{\partial t}(B_s^0 \to J/\psi\phi)} = \frac{-\eta_f\ \sin\phi_s\ \sin(\Delta m_s t)}{\cosh(\Delta\Gamma_s t/2) - \eta_f\ \cos\phi_s\ \sinh(\Delta\Gamma_s t/2)},$$

where B_s^0 and $\overline{B}_s^0$ depict the flavour of the B meson at production, η_f is the *CP* eigenvalue of the final state, and Δm_s and $\Delta\Gamma_s$ are the mass and lifetime differences between the heavy and light mass eigenstates in the $B_s^0\overline{B}_s^0$ system as introduced in the previous section.

Reconstructing the two intermediate resonances in their decays $J/\psi \to \mu^+\mu^-$ and $\phi \to K^+K^-$ provides for a clear trigger signature and clean event samples. Several factors, however, make this a challenging measurement:

- The flavour of the B meson at production has to be derived using information from the remainder of the event. This flavour tagging is not perfect and the associated mis-tag fraction dilutes the oscillation amplitude. Moreover, the dilution factor has to be known precisely in order to extract ϕ_s.
- An excellent decay time resolution is required to resolve the rapid $B_s^0 - \overline{B}_s^0$ oscillation. The finite decay time resolution leads to another dilution of the oscillation amplitude and has therefore to be known precisely in order to extract ϕ_s.
- $B_s^0 \to J/\psi\phi$ being a decay of a pseudoscalar to two vector mesons, the two final state particles can be produced with a relative angular momentum of $L = 0$, 1 or 2. The final state is not a *CP* eigenstate, $L = 1$ being *CP* odd while $L = 0$ and 2 are *CP* even. A time-dependent angular analysis of the four final state particles can statistically separate the *CP* odd and *CP* even contributions but requires large statistics.

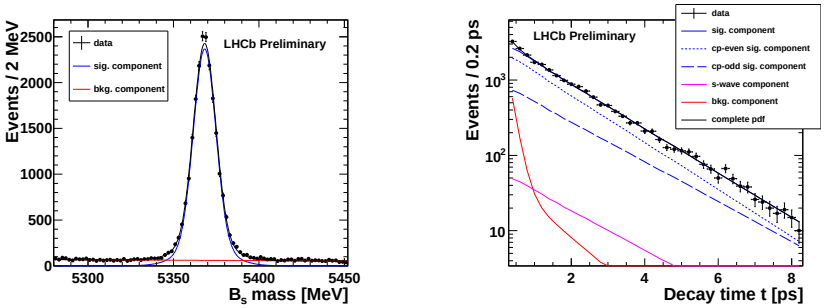

Figure 3. Left: $J/\psi K^+K^-$ invariant mass distribution of the event sample used for the ϕ_s measurement. Right: decay time distribution with fit projections overlayed.

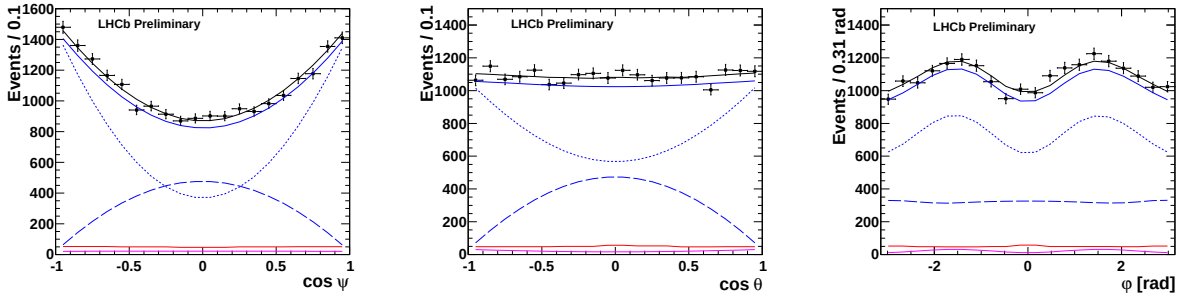

Figure 4. Distribution in the three helicity angles Ψ, θ and φ (see Ref. [23]), overlayed with projections of the time-dependent angular fit for ϕ_s. See the right plot in Fig. 3 for a legend.

- The value of $\Delta\Gamma_s$ has not been precisely measured previously and has to be determined simultaneously with ϕ_s.

Early measurements of ϕ_s performed by CDF and D0 [16, 17] indicated a possible tension with the Standard Model prediction. This tension, however, decreased and then disappeared when larger data samples were analysed [18, 19]. LHCb has performed a preliminary measurement of ϕ_s and $\Delta\Gamma_s$ using an event sample of about 21 000 $B_s^0 \to J/\psi\phi$ candidates extracted from the full 2011 data set [20][1]. The $J/\psi K^+K^-$ invariant mass spectrum is shown in Fig. 3.

A combination of opposite side tagging (OST) algorithms, described in Ref. [22], was employed to derive the initial flavour of the B meson. The OST exploits the fact that b quarks are mostly produced in quark-antiquark pairs. Flavour specific signatures from the decay of the other b hadron in the event are used to tag its flavour and it is then assumed that the flavour of the signal B meson is opposite to that of the tagging b hadron. The tagging algorithm returns a tagging decision as well as a mis-tag probability for each event, which is used to assign weights to signal events in the fit for ϕ_s. The event-by-event mis-tag probability was calibrated using a large sample of $B^\pm \to J/\psi K^\pm$ decays for which the true flavour of the signal B meson is known from the charge of the final state kaon. A global, linear calibration of the mis-tag probability is included in the fit for ϕ_s in order to absorb possible small differences between the tagging performances in $B_s^0 \to J/\psi\phi$ and in the calibration channel.

The decay time resolution was estimated event by event, using error propagation from the reconstructed momentum and decay length uncertainties. An overall calibration factor was then applied, which was determined from data using a large sample of prompt combinatorial

[1] While completing these proceedings, the measurement has been submitted for publication, see Ref. [21].

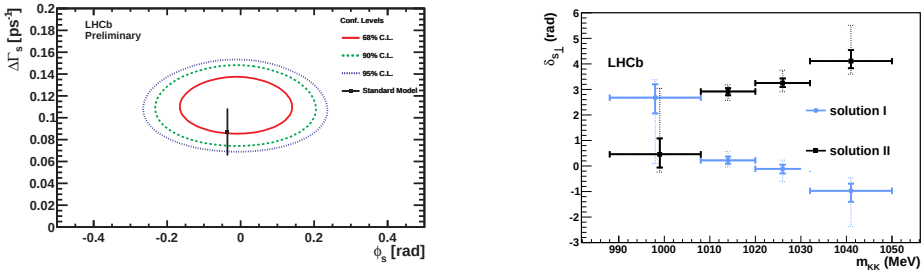

Figure 5. Left: Confidence regions in the (ϕ_s,$\Delta\Gamma_s$) plane, where only statistical uncertainties are included. Right: Measured phase difference $\delta_S - \delta_\perp$ for selected $B_s^0 \to J/\psi K^+K^-$ candidates in four bins of the K^+K^- invariant mass around the ϕ mass. Full blue circles show the result of the fit corresponding to $\Delta\Gamma_s > 0$ and ϕ_s close to zero, full black squares show the solution corresponding to $\Delta\Gamma_s < 0$ and ϕ_s close to π.

background events formed by a true $J/\psi \to \mu^+\mu^-$ and two random kaon candidates. The effective average decay time resolution was found to be 45 fs and is therefore of the same order of magnitude as the $B_s^0 - \overline{B}_s^0$ oscillation period of ≈ 56 fs. In the fit for ϕ_s, only events with decay time larger than 0.3 fs were considered. This cut significantly reduces combinatorial background and hardly reduces the statistical sensitivity to ϕ_s.

The time-dependent angular fit was performed in the transversity basis of the $J/\psi\phi$ system as defined in Ref. [23]. The full fit function is defined in Ref. [24]. Fig. 4 shows the angular distributions in the three transversity angles, together with the fit projections separating the *CP* even and *CP* odd components. The fit projection onto the decay time distribution is shown in Fig. 3. The different lifetimes of the *CP* even and *CP* odd components are clearly visible, indicating a non-zero value of $\Delta\Gamma_s$.

The result of the fit in the (ϕ_s,$\Delta\Gamma_s$) plane is shown in Fig. 5. It presents the most precise measurement of ϕ_s and $\Delta\Gamma_s$ to date and the first observation with more than five standard deviations of a non-zero value of $\Delta\Gamma_s$. The result is in good agreement with the Standard Model prediction. The fit function is invariant under a simultaneous variable transformation $(\phi_s, \Delta\Gamma_s, \delta_\parallel, \delta_\perp) \leftrightarrow (\pi - \phi_s, -\Delta\Gamma_s, 2\pi - \delta_\parallel, -\delta_\perp)$, where $\delta_\parallel$ and $\delta_\perp$ are the strong phases of two of the transversity amplitudes of the $J/\psi\phi$ system. This ambiguity was resolved in an LHCb analysis using about 1/3 of the 2011 data set, in which the evolution of the strong phases was studied as a function of the K^+K^- invariant mass around the ϕ resonance [25]. As shown in Fig. 4, the angular fit to the $B_s^0 \to J/\psi\phi$ sample reveals a small but not negligible S wave component, for which the K^+K^- system is not produced via the ϕ resonance. The strong phase δ_S for this S wave component is expected to vary only slowly across the ϕ resonance, whereas the strong phases of the resonant $\phi \to K^+K^-$ components are expected to go through a rapid positive phase shift at the location of the resonance. Fig. 5 shows for each of the two ambiguous solutions of the fit function the resulting strong phase difference $\delta_{S\perp} = \delta_S - \delta_\perp$ in four bins of the K^+K^- invariant mass around the ϕ resonance. Solution I shows the expected decreasing trend and is selected as the physical solution with a statistical significance of 4.7 standard deviations. This is the solution corresponding to a positive value of $\Delta\Gamma_s$ and ϕ_s close to zero, i.e. the solution which is in agreement with the Standard Model prediction.

LHCb has performed an independent measurement of ϕ_s using the decay $B_s^0 \to J/\psi\pi^+\pi^-$, with 755 MeV/$c^2$ $< m(\pi^+\pi^-) <$1550 MeV/c^2 [26]. A modified Dalitz plot analysis of this decay has shown that the $\pi^+\pi^-$ system is produced predominantly in an S wave state and that the *CP* odd fraction of the $J/\psi\pi^+\pi^-$ final state is larger than 97.7 % at 95 % confidence level [27]. This simplifies the fit for ϕ_s since no angular analysis is required to separate *CP* odd

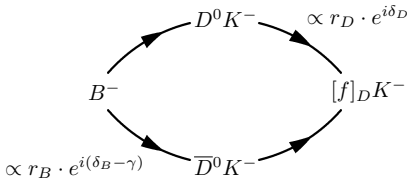

Figure 6. Illustration of the phases and ratios of magnitudes between the interfering amplitudes in tree decays $B^- \to DK^- \to [f]_D K^-$. Note that for the GLW method $r_D \equiv 1$ and $\delta_D \equiv 0$. See the text for further explanations.

and *CP* even components. On the other hand, the branching fraction for this decay is smaller than that for $B_s^0 \to J/\psi\phi$. The analysed event sample consisted of about 7400 signal candidates. A combination of the two ϕ_s analyses yields the preliminary result

$$\phi_s = -0.002 \pm 0.083(\text{stat}) \pm 0.027(\text{syst}) \text{ rad.}$$

This is the most precise determination of ϕ_s to date[2]. The precision of the measurements is limited by the statistical uncertainty. The dominant contribution to the systematic uncertainty is the assumption of no direct *CP* violation in the decay. The largest experimental uncertainty is due to angular acceptance corrections and can be further reduced with larger control channel samples.

4. Measurement of the CKM phase γ from $B^\pm \to DK^\pm$ and $B^\pm \to D\pi^\pm$ decays

The unitarity of the CKM matrix gives rise to six orthogonality relations, which can be visualised as triangles in the complex plane. The triangle derived from multiplying the first and third columns of the CKM matrix is of particular interest since its three sides are of comparable length. Its three angles are closely related to *CP* violating observables and the lengths of its sides can be measured from *CP* conserving observables. The overconstraint determination of this Unitarity Triangle provides a powerful consistency test of the CKM picture of *CP* violation.

The least well determined parameter of the Unitarity Triangle is the angle $\gamma \equiv \arg\left(-(V_{ud}V_{ub}^*)/(V_{cd}V_{cb}^*)\right)$. The CKMfitter group [28] quotes $\gamma = (66 \pm 12)^\circ$ from a global fit of CKM parameters, while the UTfit group quotes $\gamma = (72.2 \pm 9.2)^\circ$ [29].

A theoretically clean determination of γ can be derived from a combined measurement of time integrated decay rates for different $B^\pm \to DK^\pm$ tree decays. If the decay is observed in a final state $[f]_D$ that is accessible to both D^0 and $\overline{D}^0$ decays, the interference of

$$B^\pm \to D^0K^\pm \to [f]_DK^\pm \text{ and } B^\pm \to \overline{D}^0K^\pm \to [f]_DK^\pm,$$

as illustrated in Fig. 6, leads to a *CP* asymmetry that is sensitive to γ. Since the decays involve no loop diagrams, the extracted value for γ should be unaffected by possible contributions from New Physics. However, the measurements are experimentally challenging since they involve purely hadronic final states, which are difficult to trigger, and require excellent K/π separation. Moreover, branching fractions for the interesting decays are small.

Several methods using different combinations of final states $[f]_D$ have been proposed. They are usually named after the theoreticians who first proposed them.

The GLW method [30, 31] uses *CP* eigenstates such as $D^0 \to h^+h^-$, with h denoting a kaon or pion. The experimental observables are the ratios and asymmetries of time integrated decay

[2] The final result of the combined analysis, published in Ref. [21], is $\phi_s = 0.01 \pm 0.07(\text{stat}) \pm 0.01(\text{syst})$ rad.

rates

$$R_{CP+} \equiv \frac{\Gamma(B^- \to [h^+h^-]_D K^-) + \Gamma(B^+ \to [h^+h^-]_D K^+)}{\frac{1}{2}\{\Gamma(B^- \to [K^+\pi^-]_D K^-) + \Gamma(B^+ \to [K^-\pi^+]_D K^+)\}} = 1 + r_B^2 + 2\, r_B \cos\delta_B \cos\gamma$$

$$A_{CP+} \equiv \frac{\Gamma(B^- \to [h^+h^-]_D K^-) - \Gamma(B^+ \to [h^+h^-]_D K^+)}{\Gamma(B^- \to [h^+h^-]_D K^-) + \Gamma(B^+ \to [h^+h^-]_D K^+)} = \frac{2\, r_B \cos\delta_B \cos\gamma}{R_{CP+}},$$

where r_B and δ_B are the ratio of magnitudes and the relative strong phase between the two interfering decay amplitudes, respectively. The disadvantage of this method is that the decay $B^- \to \overline{D}^0 K^-$ is both CKM and colour suppressed with respect to the decay $B^- \to D^0 K^-$, leading to a small value of $r_B \approx 0.1$ and limiting the sensitivity to γ. For decays $B^\pm \to D\pi^\pm$, the CKM suppression factor is another factor 20 larger than for the case of $B^\pm \to DK^\pm$ and no sensitivity to γ is expected in these decays.

The ADS method [32, 33] tries to overcome the limitations of the GLW method by looking at quasi flavour-specific final states such as $K^-\pi^+$. The decay to this final state is Cabibbo favoured for $\overline{D}^0$ but doubly Cabibbo suppressed for D^0. The ratio of magnitudes between the D^0 and $\overline{D}^0$ decay amplitudes is $r_D \approx 0.05$, compensating for the small value of r_B and leading to similar total magnitudes for the two $B^- \to [f]_D K^-$ decay paths. Large interference is therefore possible, giving better sensitivity to γ. The price to pay is a very small total branching fraction for the doubly Cabibbo suppressed final states and the introduction of two additional parameters that have to be determined experimentally, namely r_D and the strong phase δ_D between the D^0 and $\overline{D}^0$ decay amplitudes. The experimental observables are again ratios and asymmetries of time integrated decay rates,

$$R_{ADS} \equiv \frac{\Gamma(B^- \to [K^+\pi^-]_D K^-) + \Gamma(B^+ \to [K^-\pi^+]_D K^+)}{\Gamma(B^- \to [K^-\pi^+]_D K^-) + \Gamma(B^+ \to [K^+\pi^-]_D K^+)} = r_B^2 + r_D^2 + 2\, r_B r_D \cos(\delta_B + \delta_D)\cos\gamma$$

$$A_{ADS} \equiv \frac{\Gamma(B^- \to [K^+\pi^-]_D K^-) - \Gamma(B^+ \to [K^-\pi^+]_D K^+)}{\Gamma(B^- \to [K^+\pi^-]_D K^-) + \Gamma(B^+ \to [K^-\pi^+]_D K^+)} = \frac{2\, r_B r_D \sin(\delta_B + \delta_D)\sin\gamma}{R_{ADS}}$$

The GGSZ or Dalitz-plot method [34, 35] exploits interference patterns across the Dalitz plot of self-conjugate three-body decays $D^0 \to K^0_S\pi^+\pi^-$. A rich resonance structure is observed, giving rise to large interference effects and good sensitivity to γ. However, variations of the strong phase δ_D across the Dalitz plot can be large and have to be taken into account in the extraction of γ. The associated systematic uncertainties ultimately limit the achievable precision of the measurement.

All three methods are being pursued in LHCb. Invariant mass distributions for the K^+K^- GLW mode and the suppressed ADS modes are shown in Fig. 7. Similar plots for the $\pi^+\pi^-$ GLW modes can be found in Ref. [36], where this analysis is described. The *CP* asymmetry in the $B^\pm \to DK^\pm$ GLW modes is clearly visible. Combining the two modes, the statistical significance of the asymmetry is 4.5 standard deviations. As expected, no asymmetry is seen in the $B^\pm \to D\pi^\pm$ GLW modes. Clear signals are also seen in the suppressed ADS modes and this measurement constitutes the first observation of the mode $B^\pm \to [\pi^\pm K^\mp]_D K^\pm$, with a statistical significance of about ten standard deviations. This mode displays evidence for *CP* asymmetry with a statistical significance of 4.0 standard deviations. A hint of an asymmetry is also seen in the mode $B^\pm \to [\pi^\pm K^\mp]_D \pi^\pm$, the statistical significance here being 2.4 standard deviations. The extracted results for the ratios R_{CP+} and R_{ADS} and the asymmetries A_{CP+} and A_{ADS} are listed in Ref. [36]. They are the world's most precise determinations of these parameters to date. All results are limited by statistical uncertainties. The leading systematic uncertainty on the ratios is due to the understanding of the π/K identification for the bachelor hadron, while systematic uncertainties on the asymmetries are dominated by uncertainties on production and

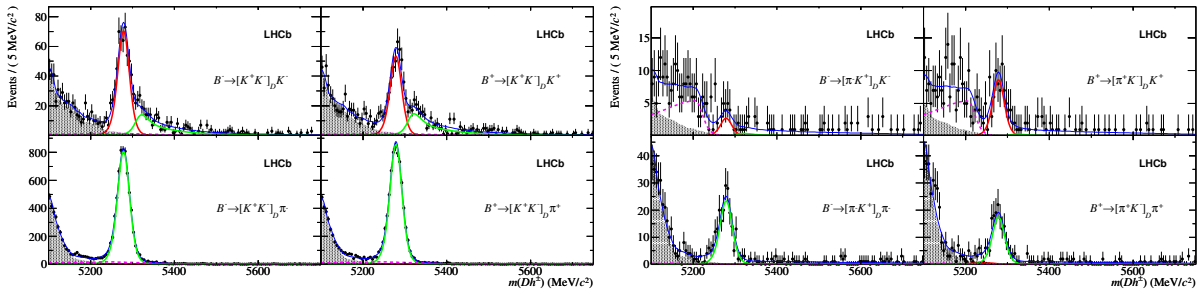

Figure 7. Invariant mass distributions for (left) the GLW modes $B^{\pm} \to [K^+K^-]_D h^{\pm}$ and (right) the suppressed ADS modes $B^{\pm} \to [\pi^{\pm}K^{\mp}]_D h^{\pm}$, where $h = K, \pi$.

detection efficiencies. These sources of uncertainties can be further reduced with larger control samples.

LHCb also performed a first GGSZ analysis [37] using D decays to $K^0_S\pi^+\pi^-$ and $K^0_S K^+K^-$. A model independent approach was chosen to avoid systematic uncertainties associated with the modelling of intermediate resonances in the D decay. Using measurements of the strong phase δ_D published [38] by the CLEO-c collaboration, the Dalitz plots were subdivided into regions (bins) in which the measured value of δ_D is approximately constant. The chosen binning scheme for the final state $K^0_S\pi^+\pi^-$ is shown in Fig. 8. The numbers $N^-_{\pm i}$ of B^- decays and $N^+_{\pm i}$ of B^+ decays in bin $\pm i$ are given by:

$$\begin{aligned} N^-_{\pm i} &\propto K_{\pm i} + (x_-^2 + y_-^2)\, K_{\mp i} + 2\sqrt{K_i K_{-i}}\,(x_- \cos(\delta_D)_{\pm i} \pm y_- \sin(\delta_D)_{\pm i}) \\ N^+_{\pm i} &\propto K_{\mp i} + (x_+^2 + y_+^2)\, K_{\pm i} + 2\sqrt{K_i K_{-i}}\,(x_+ \cos(\delta_D)_{\pm i} \mp y_+ \sin(\delta_D)_{\pm i}), \end{aligned}$$

where $K_{\pm i}$ is the number of flavour tagged D decays in bin $\pm i$ and the sensitivity to γ enters through the Cartesian parameters

$$x_{\pm} \equiv r_B \cos(\delta_B \pm \gamma) \quad \text{and} \quad y_{\pm} \equiv r_B \sin(\delta_B \pm \gamma).$$

The difference in B^- and B^+ signal yields for each bin is shown in Fig. 8 as well as the result of the fit in the ($x_{\pm}$,$y_{\pm}$) plane. The CKM angle γ is half the angle between the two vectors joining the origin and the best fit values for (x_+,y_+) and (x_-,y_-), respectively.

A combined analysis of all considered $B^{\pm} \to DK^{\pm}$ decay modes [39] yields preliminary results of

$$\gamma = (71.1^{+16.6}_{-15.7})^{\circ} \quad \text{and} \quad r_B = 0.092 \pm 0.008.$$

These results are in good agreement, and competitive, with the averages recently published by the BaBar [40] and Belle [41] collaborations.

5. *CP* violation in charmless B decays

The interference of $b \to u$ tree diagrams and $b \to s(d)$ penguin diagrams induces direct *CP* violation in two-body charmless $B^0_{(s)}$ decays. In the Standard Model, the weak phase in these decays is equal to the CKM phase γ. Possible contributions from New Physics can enter through the loop diagrams and could be revealed by comparing the weak phase measured in these decays with the value of γ measured in $B^{\pm} \to DK^{\pm}$ decays as described in the previous section. Hadronic uncertainties can be controlled by invoking U-spin symmetry (symmetry of the strong interaction under the exchange of the d and s spectator quarks) between related B^0 and B^0_s decays [42].

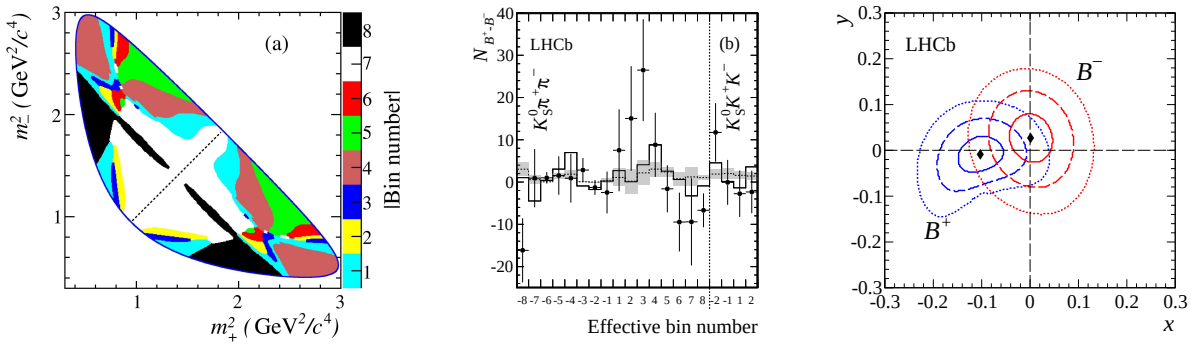

Figure 8. Left: Binning scheme chosen for the Dalitz plots in $D \to K^0_S\pi^+\pi^-$ decays. Bins above the dotted diagonal line are assigned positive bin numbers, bins below this line are assigned negative bin numbers. Middle: Difference of B^+ and B^- event yields in each bin of the Dalitz plot. The dashed line and grey shading indicate the expectation and uncertainty for the hypothesis of no *CP* violation. Right: One (solid), two (dashed) and three (dotted) standard deviation confidence levels for (x_+,y_+) (blue) and (x_-,y_-) (red). The points represent the best fit central values.

These measurements require large statistics of B^0_s decays, efficient triggers for purely hadronic final states, and excellent K/π identification to separate the different final states. LHCb is the first experiment that has the potential to apply this technique. Two approaches are pursued: measurements of the time-dependent *CP* asymmetries in decays $B^0_{(s)} \to h^+h^-$ $(h = K, \pi)$ and measurements of the time-integrated *CP* asymmetry in flavour-specific decays $B^0_{(s)} \to K^\pm\pi^\mp$. While statistical uncertainties are currently still too large to achieve sensitivity to γ, important first steps have been taken in both approaches from analyses of parts of the 2011 data set.

In the first approach, the experimental observables are the time dependent *CP* asymmetries

$$A_{CP}(t) \equiv \frac{\frac{\partial\Gamma}{\partial t}(B^0_{(s)} \to h^+h^-) - \frac{\partial\Gamma}{\partial t}(\overline{B}^0_{(s)} \to h^+h^-)}{\frac{\partial\Gamma}{\partial t}(B^0_{(s)} \to h^+h^-) + \frac{\partial\Gamma}{\partial t}(\overline{B}^0_{(s)} \to h^+h^-)} = \frac{A^{\rm dir}_{h^+h^-}\cos(\Delta m_{(s)}t) + A^{\rm mix}_{h^+h^-}\sin(\Delta m_{(s)}t)}{\cosh(\frac{\Delta\Gamma_{(s)}}{2}t) - A^{\Delta\Gamma}_{h^+h^-}\sinh(\frac{\Delta\Gamma_{(s)}}{2}t)},$$

where the sensitivity to γ enters through the direct *CP* violation amplitude $A^{\rm dir}_{h^+h^-}$. The analysis is based on about 2/3 of the 2011 data sample [43]. Similar flavour tagging algorithms as in the measurement of ϕ_s were used to determine the flavour of the $B^0_{(s)}$ at production. Samples of flavour specific decays $B^0 \to K^+\pi^-$ were used to calibrate the estimated mis-tag probabilities. The values of Δm_d and Δm_s and the sign of $\Delta\Gamma_s$ were fixed to previous LHCb measurements. The observed raw asymmetries as a function of the decay time are shown in Fig. 9. They constitute the first measurement of the $B^0 \to \pi^+\pi^-$ asymmetry at a hadron collider and the first measurement of the $B^0_s \to K^+K^-$ asymmetry ever.

In the second approach, the observables are the time-integrated *CP* asymmetries to flavour-specific final states,

$$A_{CP} \equiv \frac{\Gamma(B^0_{(s)} \to K^\pm\pi^\mp) - \Gamma(\overline{B}^0_{(s)} \to K^\mp\pi^\pm)}{\Gamma(B^0_{(s)} \to K^\pm\pi^\mp) + \Gamma(\overline{B}^0_{(s)} \to K^\mp\pi^\pm)}.$$

The invariant mass distributions obtained from an analysis of about 1/3 of the 2011 data set [44] are shown in Fig. 10. Non-zero raw asymmetries are clearly visible in both cases. Production and detection asymmetries are small and are corrected for using control channels. The measurements exclude the hypotheses of no *CP* violation with statistical significances of more than six standard deviations in the decay $B^0 \to K^+\pi^-$ and 3.2 standard deviations in the decay $B^0_s \to K^-\pi^+$.

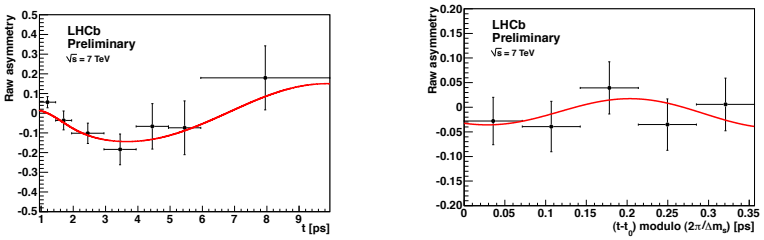

Figure 9. Time dependent *CP* asymmetry in (left) $B^0 \to \pi^+\pi^-$ and (right) $B_s^0 \to K^+K^-$.

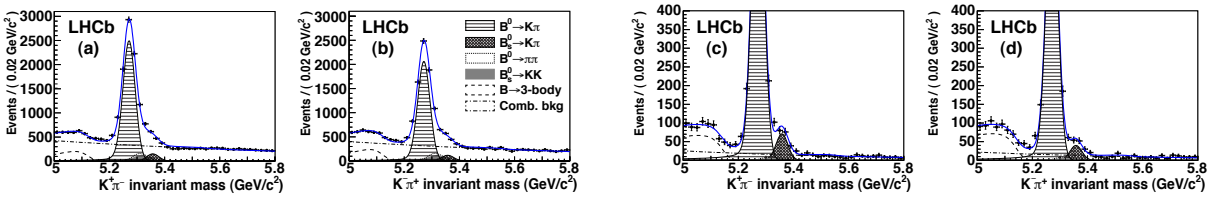

Figure 10. Invariant mass spectra for (a),(c) $K^+\pi^-$ and (b),(d) $K^-\pi^+$. Plots (a) and (b) show event selections optimized for sensitivity on $A_{CP}(B^0 \to K\pi)$, plots (c) and (d) show event selections optimized for sensitivity on $A_{CP}(B_s^0 \to K\pi)$.

These results are the first observation of *CP* violation with more than five standard deviations at a hadron collider and the first evidence with more than three standard deviations for *CP* violation in the B_s^0 system, respectively.

6. Summary and Outlook: The LHCb upgrade

The LHCb experiment has performed oustandingly well during the first three years of LHC operation. Many competitive and world-best measurements have been obtained from the analysis of the 2011 data set, corresponding to an integrated luminosity of 1.0 fb^{-1} of pp collisions collected at a centre of mass energy of 7 TeV. All results are dominated by statistical uncertainties and in most cases the leading systematic uncertainties can be further reduced by using larger samples of control channels. An additional 2 fb^{-1} of good quality data have been collected in 2012 and are being analysed. After the first long shutdown (LS1) of the LHC, the machine will resume operation at a centre of mass energy of 13 TeV. This will roughly double the heavy quark production cross sections. Assuming that the LHC will deliver about 5 fb^{-1} to LHCb during the run following LS1, the accumulated statistics will have increased by more than a factor ten by the time of the second long LHC shutdown (LS2), which is scheduled for 2018-2019.

The LHCb collaboration is preparing a comprehensive upgrade of the detector and its readout, to be installed and commissioned during LS2. The physics case and details of the upgrade plans are described in Ref. [47] and in the Letter of Intent [48] and the Framework Technical Design Report [49] for the upgrade. The upgrade plan contains two main components: to prepare the detector for operation at a five times increased instantaneous luminosity and to read out the full detector at the LHC bunch crossing rate of 40 MHz. By overcoming the limitations of the current hardware based trigger level, the 40 MHz readout will gain a factor of two in trigger efficiencies for b hadron decays to fully hadronic final states. Together with the increased heavy quark production cross section, the expected gains in event yields per year, compared to 2011, are a factor 10 in channels involving muons in the final state and a factor 20 in channels to fully hadronic final states. In total, the upgraded experiment is expected to collect an integrating luminosity of 50 fb^{-1} over 10 years of operation.

References

[1] A. A. Alves, Jr. *et al.* [LHCb Collaboration], JINST **3** (2008) S08005.
[2] E. Grauges Pous *on behalf of the LHCb Collaboration*, "Testing the Standard Model with rare decays at the LHCb," LHCb-PROC-2013-020.
[3] N. Cabibbo, Phys. Rev. Lett. **10** (1963) 531.
[4] M. Kobayashi and T. Maskawa, Prog. Theor. Phys. **49** (1973) 652.
[5] B. Aubert *et al.* [BaBar Collaboration], Phys. Rev. D **79** (2009) 072009 [arXiv:0902.1708 [hep-ex]].
[6] I. Adachi, H. Aihara, D. M. Asner, V. Aulchenko, T. Aushev, T. Aziz, A. M. Bakich and A. Bay *et al.*, Phys. Rev. Lett. **108** (2012) 171802 [arXiv:1201.4643 [hep-ex]].
[7] A. Lenz, arXiv:1205.1444 [hep-ph].
[8] B. Aubert *et al.* [BaBar Collaboration], Phys. Rev. Lett. **96** (2006) 251802 [hep-ex/0603053].
[9] B. Aubert *et al.* [BaBar Collaboration], hep-ex/0607091.
[10] E. Nakano *et al.* [Belle Collaboration], Phys. Rev. D **73** (2006) 112002 [hep-ex/0505017].
[11] V. M. Abazov *et al.* [D0 Collaboration], Phys. Rev. D **86** (2012) 072009 [arXiv:1208.5813 [hep-ex]].
[12] V. M. Abazov *et al.* [D0 Collaboration], Phys. Rev. D **84** (2011) 052007 [arXiv:1106.6308 [hep-ex]].
[13] LHCb Collaboration, LHCb-CONF-2012-022.
[14] R. Aaij *et al.* [LHCb Collaboration], Phys. Lett. B **713** (2012) 186 [arXiv:1205.0897 [hep-ex]].
[15] J. Charles, O. Deschamps, S. Descotes-Genon, R. Itoh, H. Lacker, A. Menzel, S. Monteil and V. Niess *et al.*, Phys. Rev. D **84** (2011) 033005 [arXiv:1106.4041 [hep-ph]].
[16] The CDF Collaboration, CDF public note CDF/ANAL/BOTTOM/PUBLIC/9458.
[17] V. M. Abazov *et al.* [D0 Collaboration], Phys. Rev. Lett. **101** (2008) 241801 [arXiv:0802.2255 [hep-ex]].
[18] T. Aaltonen *et al.* [CDF Collaboration], Phys. Rev. Lett. **109** (2012) 171802 [arXiv:1208.2967 [hep-ex]].
[19] V. M. Abazov *et al.* [D0 Collaboration], Phys. Rev. D **85** (2012) 032006 [arXiv:1109.3166 [hep-ex]].
[20] LHCb Collaboration, LHCb-CONF-2012-002.
[21] R. Aaij *et al.* [LHCb Collaboration], arXiv:1304.2600 [hep-ex].
[22] R. Aaij *et al.* [LHCb Collaboration], Eur. Phys. J. C **72** (2012) 2022 [arXiv:1202.4979 [hep-ex]].
[23] A. S. Dighe, I. Dunietz, H. J. Lipkin and J. L. Rosner, Phys. Lett. B **369** (1996) 144 [hep-ph/9511363].
[24] R. Aaij *et al.* [LHCb Collaboration], Phys. Rev. Lett. **108** (2012) 101803 [arXiv:1112.3183 [hep-ex]].
[25] R. Aaij *et al.* [LHCb Collaboration], Phys. Rev. Lett. **108** (2012) 241801 [arXiv:1202.4717 [hep-ex]].
[26] R. Aaij *et al.* [LHCb Collaboration], Phys. Lett. B **713** (2012) 378 [arXiv:1204.5675 [hep-ex]].
[27] R. Aaij *et al.* [LHCb Collaboration], Phys. Rev. D **86** (2012) 052006 [arXiv:1204.5643 [hep-ex]].
[28] J. Charles *et al.* [CKMfitter Group Collaboration], Eur. Phys. J. C **41** (2005) 1 [hep-ph/0406184], updated results and plots available at: http://ckmfitter.in2p3.fr.
[29] D. Derkach [UTfit Collaboration], arXiv:1301.3300 [hep-ph].
[30] M. Gronau and D. London, Phys. Lett. B **253** (1991) 483.
[31] M. Gronau and D. Wyler, Phys. Lett. B **265** (1991) 172.
[32] D. Atwood, I. Dunietz and A. Soni, Phys. Rev. Lett. **78** (1997) 3257 [hep-ph/9612433].
[33] D. Atwood, I. Dunietz and A. Soni, Phys. Rev. D **63** (2001) 036005 [hep-ph/0008090].
[34] A. Giri, Y. Grossman, A. Soffer and J. Zupan, Phys. Rev. D **68** (2003) 054018 [hep-ph/0303187].
[35] A. Poluektov *et al.* [Belle Collaboration], Phys. Rev. D **70** (2004) 072003 [hep-ex/0406067].
[36] R. Aaij *et al.* [LHCb Collaboration], Phys. Lett. B **712** (2012) 203 [Erratum-ibid. B **713** (2012) 351] [arXiv:1203.3662 [hep-ex]].
[37] R. Aaij *et al.* [LHCb Collaboration], Phys. Lett. B **718** (2012) 43 [arXiv:1209.5869 [hep-ex]].
[38] J. Libby *et al.* [CLEO Collaboration], Phys. Rev. D **82** (2010) 112006 [arXiv:1010.2817 [hep-ex]].
[39] LHCb Collaboration, LHCb-CONF-2012-032.
[40] J. P. Lees *et al.* [BaBar Collaboration], Phys. Rev. D **87** (2013) 052015 [arXiv:1301.1029 [hep-ex]].
[41] K. Trabelsi [Belle Collaboration], arXiv:1301.2033 [hep-ex].
[42] R. Fleischer, Eur. Phys. J. C **52** (2007) 267 [arXiv:0705.1121 [hep-ph]].
[43] LHCb Collaboration, LHCb-CONF-2012-007.
[44] R. Aaij *et al.* [LHCb Collaboration], Phys. Rev. Lett. **108** (2012) 201601 [arXiv:1202.6251 [hep-ex]].
[45] LHCb Collaboration, LHCb-CONF-2012-018.
[46] LHCb Collaboration, LHCb-CONF-2012-028.
[47] R. Aaij *et al.* [LHCb Collaboration], arXiv:1208.3355 [hep-ex].
[48] LHCb Collaboration CERN/LHCC-2011-001.
[49] LHCb Collaboration, CERN/LHCC-2012-007.